CHEMICAL ENGINEERING TRANSACTIONS
VOL. 116, 2025
A publication of AIDIC
The Italian Association of Chemical Engineering
Online at www.cetjournal.it
Guest Editors: Bruno Fabiano, Valerio Cozzani

ISBN 979-12-81206-18-2; **ISSN** 2283-9216
DOI: 10.3303/CET25116060

Thermal Hazard Study on The Synthesis of 3-Amino-4-nitrofurazan

Liping Chen[a], Jiayu Lyu[b], Juan Zhou[c], Meiling Liu[a]*, Zichao Guo[a], Wanghua Chen[a]

[a] Department of Safety Engineering, School of Safety Science and Engineering, Nanjing University of Science and Technology, Nanjing, Jiangsu, 210094, China
[b] Analysis and Testing Center, Institute of Zhejiang University – Quzhou, Quzhou, Zhejiang, 324003, China
[c] China Safety Technology Research Academy of Ordnance Industry, Beijing, 100053, China
liumeilingfighting@163.com

The synthesis of 3-amino-4-nitrofurazan (ANF), a critical precursor for various monofurazan derivatives, involves the oxidation of 3,4-diaminofurazan (DAF) using an oxidizing system of CH_3SO_3H-H_2O_2-Na_2WO_4. This complex process produces two primary outcomes: the desired product ANF and a by-product, 3,3'-diamino-4,4'-azofuroxide (DAOAF). To evaluate the thermal hazards associated with this reaction, reaction calorimetry (RC1) was utilized to study the thermal behavior, followed by separation, washing, extraction, evaporation, and drying of the final reaction mixture, resulting in two solid products: a filter cake and the dried filtrate. The yields of ANF and DAOAF were quantified through HPLC analysis. Kinetic parameters were derived using a five-step reaction model based on heat generation rate data. Findings indicate that the fourth reaction step, responsible for ANF formation, demonstrated the highest heat release at 599.9 kJ·mol^{-1} with an activation energy of 93.0 kJ·mol^{-1}. The Maximum Temperature of Synthesis Reaction (MTSR) was established at 55°C, while adiabatic calorimetry suggested limited thermal stability, with a T_{D24} of 23°C. Consequently, Dr. Stoessel's thermal runaway classification was expanded from five to six classes to assess the thermal risks better, categorizing the oxidation reaction as Class 6.

1. Introduction

3,4-diaminofurazan (DAF) is a fundamental compound in the furazan family, serving as a precursor for many furazan-based energetic materials, including 3-amino-4-nitrofurazan (ANF). ANF is an important intermediate of synthesizing furazan-based energetic materials, which is obtained by oxidizing one of the amino groups in DAF to a nitro group. The weak basicity of the amino groups on the furazan ring, coupled with the electronic effects of the furazan ring, severely passivates the amino groups. Therefore, the only way to introduce a nitro functional group onto the furazan ring is through oxidation of the amino group. Moreover, the oxidation of amino furazan requires relatively harsh conditions (Andrianov and Eremeev, 1985). The earliest method of ANF synthesis was mentioned by Russian scholars Novikova et al. (1994), who suggested using a combination of hydrogen peroxide and sulfuric acid for DAF oxidation to ANF. In 2007, Zhang et al. (2007) noted that the use of concentrated sulfuric acid made temperature control difficult, increasing the likelihood of side reactions and even preventing the formation of the target product. Therefore, they employed a Na_2WO_4-$H_2C_2O_4$ co-catalyst system at 30 °C, achieving an ANF yield of 33.7%. In 2008, Li et al. (2008) for the first time used methane sulfonic acid (CH_3SO_3H) as the reaction medium to form a new oxidizing system, CH_3SO_3H-H_2O_2- Na_2WO_4, achieving an ANF yield of 67%. In 2010, Wu (2010) synthesized ANF using a mixed oxidizing system based on Li's work(2008), finding the optimal reaction temperature to be 30°C and the best molar ratio of sodium tungstate to DAF as 1:1, which resulted in the highest ANF yield.
In summary, current research on the synthesis of ANF has largely focused on optimizing synthesis methods to improve yield. However, as ANF is a nitro-containing compound with high energy, it poses thermal risks. Many studies indicate that hydrogen peroxide and its oxidizing systems can decompose at room temperature (Zhang, 2020), and that materials like stainless steel can catalyze these reactions (Gan, 2019). Thus, the nature of the

Paper Received: 19 November 2024; Revised: 28 February 2025; Accepted: 22 March 2025
Please cite this article as: Chen L., Lyu J., Zhou J., Liu M., Guo Z., Chen W., 2025, Thermal Hazard Study on the Synthesis of 3-Amino-4-nitrofurazan, Chemical Engineering Transactions, 116, 355-360 DOI:10.3303/CET25116060

reactants and products in this synthesis process implies a potential for thermal hazards. Therefore, this study focuses on the risk of thermal runaway in the synthesis process of ANF.

2. Reagents, equipment and test conditions

This study bases its thermal runaway risk analysis on the ANF synthesis process proposed by Wu (2010).

2.1 Reagents and samples

The main reagents or samples used include:
(1) DAF, a pale yellow flocculent solid, purchased from Shanghai Bide Pharmaceutical Technology Co, Ltd, with a purity of 96%.
(2) 30% hydrogen peroxide, a clear liquid, obtained from Sinopharm Chemical Reagent Co, Ltd.
(3) Sodium tungstate (Na_2WO_4) , white solid particles, purchased from Maclin Biochemical Technology Co, Ltd, with a purity of 99.5%.
(4) Methane sulfonic acid, a colorless liquid, purchased from Maclin Biochemical Technology Co, Ltd, with a purity of 98%.
(5) Product liquid, a heterogeneous liquid sample taken maintaining the phase ratio after the synthesis reaction.

2.2 Equipment and software

The equipment and software used are listed in Table 1.

Table 1: Equipment and software information

Name abbreviation	Information
RC1e	METTLER TOLEDO, equipped with a 500 ml glass reactor
DSC1	METTLER TOLEDO, disposable gold-plated crucible
esARC	THT Company, Hastelloy bomb
HPLC	Shandong Wukong Instrument Co., Ltd, model K2025, mobile phase ratio is acetonitrile: ammonium acetate = 55:45, UV wavelength 214nm
TSS	CISP Company, using RCpro and Deskpro modules

2.3 Reaction calorimetry experiments

According to the procedures proposed by Wu (2010), reaction conditions in the RC1 test were set as follows: at 10°C, 132 ml of a 30% hydrogen peroxide solution and 10.9 g of sodium tungstate were sequentially added to the reactor, followed by heating to 30°C (to conduct kinetic calculations, reactions at 25°C and 35°C were also carried out). Pre-prepared mixtures of 6.6 g DAF and 43 ml methane sulfonic acid were then added to the reactor at a rate of 1 ml min^{-1}, with stirring maintained for 3.5 h post addition. After reaction termination, the reaction mixture was poured into ice water, precipitating solids, which were filtered, washed, and dried. The main component was 3,3'-diamino-4,4'-oxidized azofurazan (DAOAF). The filtrate was extracted with dichloromethane and the organic phase was concentrated under reduced pressure to yield pale yellow crystals primarily composed of ANF. HPLC was used to analyze both filter cake and rotary evaporation products, employing an external standard method to determine ANF and DAOAF contents.

2.4 Reaction pathways of DAF oxidation

Wang (2018) suggested pathways for DAF oxidation to yield ANF and DAOAF, as illustrated in Figure 1.

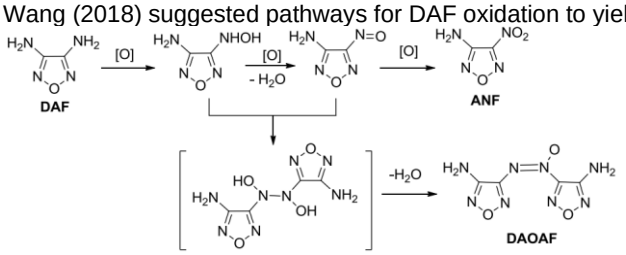

Figure 1: Synthesis pathways of ANF and DAOAF (Wang, 2018)

DAF is initially oxidized to form hydroxylamine intermediates, which further oxidize into nitroso furazan. Further oxidation yields nitrofurazan (ANF), while nitroso and hydroxylamine intermediates couple to form oxidized azofurazan. In this process, sodium tungstate acts as a catalyst, enhancing the reactivity of hydrogen peroxide.

Methane sulfonic acid reacts with hydrogen peroxide to form peroxymethanesulfonic acid, which acts as the selective oxidant, increasing DAF conversion to ANF.

3. Results and discussion

3.1 Phenomena and Exothermic Characteristics in ANF Synthesis

Upon mixing sodium tungstate with hydrogen peroxide, a transparent orange-yellow solution formed. Adding DAF and methane sulfonic acid transformed the solution from orange-yellow to emerald green, eventually changing to dark green while small amounts of yellow solid particles floated on the surface. As the reaction progresses, the solution transitioned from green to yellow, with increasing solid particulates, culminating in an orange-yellow suspension. The exothermic rate and temperature curves for the DAF oxidation process are depicted in Figure 2, with data tabulated in Table 2. The initial q_r curve instability corresponds to the addition phase, stabilizing once the reactive components fully interact, trending upward slowly till reaching a steady state post-addition, indicative of decelerated reaction rates. Post-completion, q_r decreases.
The data shows that total heat increases with processing temperature, averaging 81kJ, with a 30°C process temperature yielding a maximal 75% ANF and minimal DAOAF yield (see Table 2).

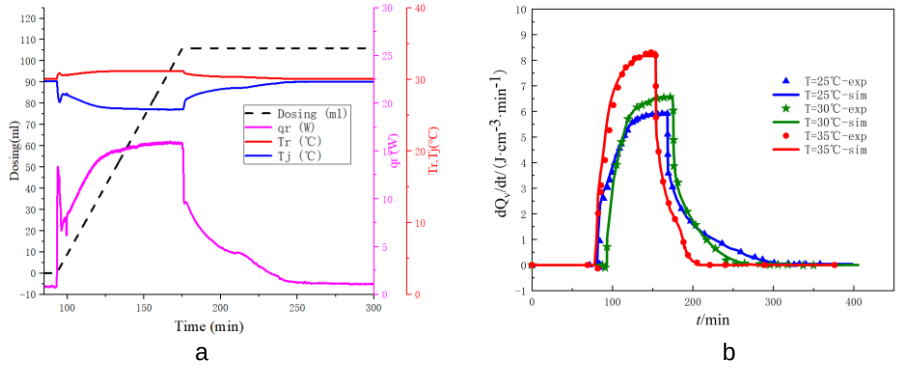

Figure 2 Experimental curves during ANF synthesis by RC1e. （a）Test curves of the reaction at 30 °C, （b）Fitting curves of the heat generation rate at different temperatures

Table 2: RC1e experimental results for ANF synthesis at various temperatures

T_p(℃)	c_{p1} (J·g^{-1}·K^{-1})	c_{p2} (J·g^{-1}·K^{-1})	Q_{tot} (kJ)	Yield of ANF	Yield of DAOAF
25	3.642	2.535	79	0.60	0.21
30	3.686	2.594	80	0.75	0.17
35	3.915	2.718	84	0.67	0.23

3.2 Reaction kinetics of ANF synthesis

The oxidation of DAF to synthesize ANF involves complex reactions. Previous methods used to calculate the maximum temperature achievable by the desired synthetic reaction (MTSR) made the simplifying assumption of a single-step reaction, potentially introducing significant errors in thermal safety assessments for multi-step reactions. Considering that reactants are dissolved in the liquid phase, it is feasible to obtain accurate kinetic parameters through appropriate modelling and fitting of calorimetric data, and ultimately provide more accurate MTSR.
Initially, the RCpro module of TSS software was employed to process RC1e experiment data across various process temperatures, such as baseline correction, integration, deconvolution, and elimination of irrelevant data. Subsequently, the Deskpro module was utilized to construct a model for the ANF synthesis process and calculate reaction kinetics. Proper reaction modelling is essential before fitting kinetics. Based on the reaction pathways illustrated in Figure 1, the reaction equations are structured as follows:

Step 1: $H_2O_2+CH_3SO_3H \rightarrow H_2O+CH_3SO_4H$
Step 2: $C_2H_4N_4O+CH_3SO_4H \rightarrow C_2H_4N_4O_2+CH_3SO_3H$
Step 3: $C_2H_4N_4O_2+CH_3SO_4H \rightarrow C_2H_2N_4O_2+CH_3SO_3H+H_2O$
Step 4: $C_2H_2N_4O_2+3CH_3SO_4H \rightarrow C_2H_2N_4O_3+3CH_3SO_3H$
Step 5: $C_2H_2N_4O_2+ C_2H_4N_4O_2 \rightarrow C_4H_4N_8O_3+ H_2O$

Where CH_3SO_3H is the molecular formula of methane sulfonic acid, CH_3SO_4H is the molecular formula of peroxymethanesulfonic acid, $C_2H_4N_4O$, $C_2H_4N_4O_2$, $H_2N_4O_2$, $C_2H_2N_4O_3$, $C_4H_4N_8O_3$ are the molecular formulas of DAF, 3-Amino-4-Hydroxylamino Furazan, 3-Amino-4-Nitroso Furazan (ANSF), ANF, DAOAF, respectively. Sodium tungstate and hydrogen peroxide form a complex before adding DAF; hence, H_2O_2 represents the hydrogen peroxide-tungstate complex. The corresponding reaction rate can be expressed by the Arrhenius equation, in which R1 and R2 represent reactant 1 and reactant 2, respectively.

$$r_i = A\exp(-E/RT)[R1]^{n_1}[R2]^{n_2} \quad (1)$$

Nonlinear fitting methods such as the least squares approach were applied in TSS to minimize residuals between experimental and fitted values. The fitting quality was evaluated using the square residual sum, and the optimization was carried out using tensor-based normal models and the implicit Runge-Kutta integration method, with iteration limits set to 100 and an error threshold of 0.001. The kinetic parameters were derived by determining the lowest weighted sum of square residuals.

The measured q_r data was fitted. Initial feeding caused substantial reaction fluctuations and sensor response delays, leading to early q_r curve disturbance. These disturbances were corrected before kinetic fitting. The finalized fitting results and kinetic parameters are illustrated in Figure 2(b) and Table 3, respectively.

Table 3: Fitting results of the kinetic parameters

Step	E (kJ·mol^{-1})	ln(A)	n_1	n_2	Q_n (kJ·mol^{-1})
1	96.7	37.6	1.14	2.32	12.7
2	60.2	22.6	1.73	0.36	193.7
3	93.9	31.3	1.15	1.21	124.0
4	93.0	27.7	0.71	0.71	559.9
5	119.0	41.7	1.22	0.85	110.2

3.3 Calculation of MTSR

$\Delta T_{ad,rx}$ of the synthesis at 30°C can be calculated by equation (2):

$$\Delta T_{\mathrm{ad,rx}} = \frac{Q_{tot}}{M_{rf} \times C_p} = \frac{80}{0.2637 \times 3.14} = 97℃ \quad (2)$$

With hydrogen peroxide excess, gradual DAF accumulation is inevitable, peaking upon complete addition. MTSR based on the previous calculation method (Stoessel, 2008) can be obtained as:

$$MTSR1 = T_p + \Delta T_{\mathrm{ad,rx}} \cdot X_{ac,max} \cdot \frac{M_{rf}}{M_{r,max}} = 49℃ \quad (3)$$

Where $X_{ac,max}$ is considered as the accumulation degree at the end of feeding.

MTSR1 is calculated without considering temperature-induced competitive reaction shifts. Therefore, established kinetic models were used to predict 30°C reaction and cooling failure scenarios precisely (Figure 3).

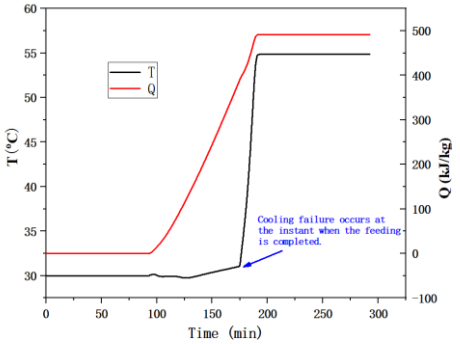

Figure 3: Temperature and heat predicted curve assuming cooling failure occurs at the end of dosing based on the kinetic model.

The cooling capacity was set as heat removal analogous to RC1 trials first, and hypothetical zero heat removal (cooling failure) at the end of dosing shows sustained temperature rise till reaction completion, peaking at 55°C (MTSR2) with 491 kJ·kg^{-1} heat generation against a normal 303 kJ·kg^{-1}. A 20-minute post-failure period to maximal temperature highlights rapid exothermic steepness.

3.4 Thermal runaway risk classification method

Thermal runaway studies encompass material thermal stability and intrinsic reaction characteristics. Gygax (1988) defined worst-case scenarios for runaway potential desired primary reactions, innovating the MTSR parameter for cumulative heat studies. Building upon this, Stoessel (2008) proposed a runaway scenario in case of cooling failure and established Tp, MTSR, MTT, and T_{D24} as evaluative benchmarks for process safety risk categorization (Figure 4a). Simultaneously, Grewer (1994) elucidated primary-secondary reaction interactions with Ts as the decomposition benchmark (Figure 4b).
Case 1: Ts>MTSR indicates relative process safety barring thermal influences.
Case 2: Tp < Ts < MTSR suggests intermediates' potential degradation risk, exacerbated by high secondary reaction exotherms.
Case 3: Ts approximates or falls below Tp, challenging secure operation without compounded reaction exothermic safety measures.

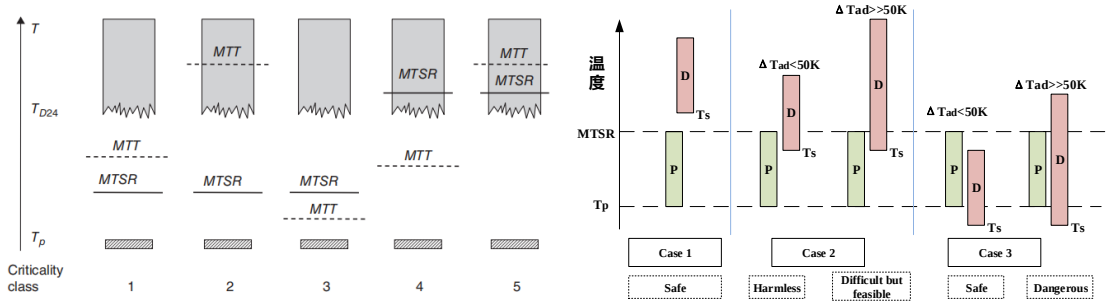

Figure 4: Reaction Classification, (a) Criticality classes of scenario proposed by Stoessel, (b) Relationship between primary reaction (P) and secondary decomposition reaction (D)

The risk classification proposed by Dr. Stoessel (Figure 5a) aligns levels 1-3 with Case 1 and levels 4-5 with Case 2, without specific mention of Case 3. Building on this, class 6 is proposed here: Tp ≥T_s (T_{D24}). And the thermal runaway risk of the synthesis of ANF will be evaluated based on this 6-class thermal hazard classification.

3.5 Thermal Decomposition Evaluation

The post-reaction product liquid was tested by esARC to assess runaway risk (Figure 5a).

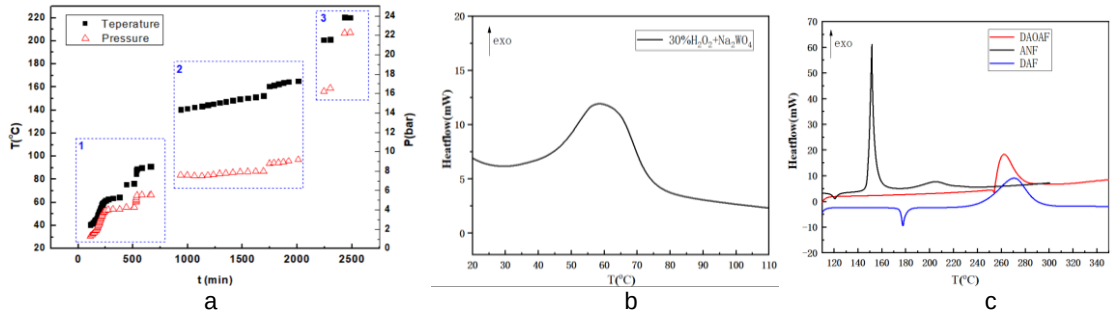

Figure 5: Adiabatic and DSC Test Results of different samples, (a) Exothermic Cycle Temp/Pressure-Time Curve of product liquid under adiabatic condition, (b) DSC curve of 30% H_2O_2+Na_2WO_4(8°C/min), (c) DSC curves of DAOAF, ANF and DAF(8°C/min).

Heterogeneous samples was tested by esARC tests with 1.014g samples, average 3.14J·g^{-1}·K^{-1} specific heat, phi of 2.89. The result presents three exothermic stages, The initial decomposition onsets at 40.7°C, with 92.6°C endpoint, and 144°C corrected adiabatic temperature rise, correlating with the decomposition of the hydrogen peroxide oxidation system. The second decomposition onsets at 140.4°C, terminating at 165.35°C, releasing 72.0°C corrected adiabatic heat. Resultant primary exotherm prompted by auto-decomposition preloads, prompting subsequent releases. The third plateau is triggered at about 200°C. Secondary decomposition notable post-load thermal elevation, reflected by T_{D24} extrapolations computing to 23°C.

3.6 Thermal Runaway Assessment

$\Delta T_{ad,rx}$ of the synthesis at 30°C is 97°C. High heat conclusively signals runaway risk while combining material decompositions implies further safe margin requisites. MTSR1=49°C, MTSR2=55°C, T_{D24}=23°C, T_p=30°C, reveal $T_{D24} < T_p <$ MTSR, suggesting recombining material with unstable bulk hydrogen peroxide accentuates decomposition preludes expanding operations danger to a sixth-tier classification.

4. Conclusion

The synthesis of ANF from DAF is an intricately exothermic process, prone to thermal buildup post-addition under obvious competitive side and decomposition reaction, especially amid cooling failure risks. Higher temperature testing alongside kinetic computational modeling can discern reaction heat influences, refining MTSR estimates.

Hydrogen peroxide-based oxidation demonstrates systemic stability sensitivity, synchronizing synthesis and decomposition ventures. In cooling failure contexts, temperature escalation is imminent, advocating advanced runaway classification identifying sixth-tier synthesis with heightened preparatory in-process cooling reliability to avert escalation.

Nomenclature

A – pre-exponential factor, min^{-1}
c_p – specific heat capacity, $J \cdot g^{-1} \cdot K^{-1}$
E – activation energy, $kJ \cdot mol^{-1}$
MTSR- Maximal Temperature attainable by runaway of the desired Synthetic Reaction, °C
M_{rf} – the mass of the reaction mixture at the end of the feed, kg
$M_{r,\ max}$ – the mass of the reaction mixture at the instant of maximum accumulation, kg
MTT - Maximum temperature for technical reasons, °C
n – reaction order
Q_{tot} – heat of the reaction tested by RC1, kJ
Q_n – molar reaction heat, $kJ \cdot mol^{-1}$
Q_v – volume reaction heat, $J \cdot ml^{-1}$
q_r – heat flow or heat generation rate, W
ΔT_{ad} – adiabatic temperature rise, °C
T_{D24} – Temperature at which TMR_{ad} (Time to maximum rate under adiabatic) of the decomposition= 24 hours, °C
T_p – process temperature, °C
T_s – onset temperature of the secondary reaction, °C, e.g. T_{D24}
$X_{ac,\ max}$ – the maximum degree of accumulation

Acknowledgments

This research was supported by the National Natural Science Foundation of China (No. 22278226). The authors gratefully acknowledge this supports.

References

Andrianov V. G., Eremeev A. V., 1985, ChemInform Abstract: Aminofurazans (Reviews). Chemischer Informationsdienst, 16(7).

Gan X. Y., Research on thermal stability of hydrogen peroxide and benzoyl peroxide with impurities, Master Thesis. Nanjing University of Science and Technology, 2019.

Grewer T., 1994, Thermal hazards of chemical reactions. Elsevier, Amsterdam

Gygax R. 1988, Chemical reaction engineering for safety. Chemical Engineering Science, 43(8): 1759-1771

Li H. Z., Zhou X. Q., Li J. S., Huang M., 2008, Synthesis of 3-Amino-4-nitrofurazan and 3,3-Dinitro-4，4-azofurazan, Chinese Journal of Organic Chemistry, 28(9): 1646-1648.

Novikova T. S., Mel'Nikova T. M., Kharitonova O. V., Kulagina V. O., Aleksandrova N. S., Sheremetev A. B., Pinina T. S., Khmel’nitskii L. I., Novikov S. S., 1994, An Effective Method for the Oxidation of Aminofurazans to Nitrofurazans. Mendeleev Communications, 4(4): 138-140.

Stoessel F., 2008, Thermal safety of chemical processes——risk assessment and process design. 1st ed. Wiley-VCH, The FEDERAL Republic of Germany:

Wang X. X., Studies on the Hundred Grams-scale Preparation and Technology of High-purity DAOAF. Master Thesis. Southwest University of Science and Technology, 2018.

Wu C., Research on the Synthesis of 3,4-Diaminofurazan and Its Derivatives. Master Thesis. Nanjing University of Science and Technology, 2010.

Zhang M. Y., Thermal Risk Assessment on Oxidation Process of 3,4-Dia minofurazan, Master Thesis. Nanjing University of Science and Technology, 2020.

Zhang J. Q.，Zhang W., Zhu H. Wang C. H., Wang Y. W., 2007, Synthesis of 3-Amino-4-nitroflIrazan by an Improved Method, Chinese Journal of Energetic Materials, 15(6): 577-580.